TEMPERATURE MEASUREMENTS OF SINGLE COAL PARTICLES DURING THE EARLY STAGES OF HEATING AND DEVOLATILIZATION

Daniel J. Maloney, Esmail R. Monazam, Steven D. Woodruff and Larry O. Lawson
Morgantown Energy Technology Center
P. O. Box 880
Morgantown, West Virginia 26507-0880

Keywords: coal devolatilization, temperature measurement, combustion

ABSTRACT

Unique instrumentation was applied to measure changes in coal particle size and temperature during the early stages of heating and devolatilization. The system incorporated an electrodynamic balance and a pulsed radiation source with a high-speed photodiode array and single wavelength radiation pyrometer. Single coal and carbon particles were pulse heated to simulate the rapid heating rates experienced in high intensity combustion environments (10^5 K/s). Measured temperature histories for 135 μm diameter carbon spheres were in excellent agreement with theoretical predictions of the temperature response of radiatively heated spheres using heat capacity and thermal conductivity property correlations commonly applied in modeling coal devolatilization and combustion. Measured temperature histories of 115 μm coal particles, however, greatly exceeded (on the order of 50 percent) theoretical predictions of the temperature response using the same assumptions and property correlations. Potential causes for the high heating rates observed include uncertainty in assigning thermodynamic and heat transfer properties as well as failure to account for particle shape factors. It is concluded that heat transfer analyses employing spherical particle assumptions and commonly used coal property correlations can lead to significant underestimation of temperature histories and corresponding errors in associated devolatilization rates.

INTRODUCTION

The large discrepancies in observed temperature sensitivities for coal devolatilization are well documented.[1,2] with variations in reported rate constants at a given temperature of several orders of magnitude being common. These variations can in large part be attributed to the experimental techniques used to study rapid devolatilization because estimation and/or measurement of coal particle temperatures in these systems is difficult. Recent attempts to overcome these limitations have concentrated on in-situ temperature measurement or careful characterization of heat transfer fields. For example, Solomon and coworkers[3,4] developed and applied an FTIR emission/transmission technique to measure average temperatures for clouds of devolatilizing coal particles in an entrained flow reactor. Fletcher[5,6] recently reported using a two-color particle sizing pyrometer to characterize the temperature history of single devolatilizing particles in an entrained flow reactor. Friehaut and Proscia[7] performed a detailed characterization of the temperature rise in a screen heater system which was then applied to study rapid devolatilization. Results from these investigations suggest that coal devolatilization rates may be significantly faster and have a stronger temperature sensitivity than implied from many previous studies. The importance of accurate temperature measurements in future devolatilization studies is clear.

In the present paper a novel system is described for monitoring rapid changes in particle size and temperature during coal devolatilization at heating rates representative of high intensity combustion environments (on the order of 10^5 K/s).

The objective was to time and temperature resolve tar evolution and particle swelling that accompany devolatilization and thereby provide data needed to develop more accurate predictions of coal combustion behavior. Initial measurements are reported along with a discussion of the implications for predicting coal devolatilization in combustion systems.

EXPERIMENTAL

Single coal or carbon particles were statically charged and captured in an electrodynamic balance (EDB). Details of the design and operation of the EDB system are published elsewhere.[8,9] The captured particles were balanced at the EDB null position and then heated radiatively from opposite sides by well characterized pulsed Nd:YAG laser beams of equal intensity. Delivered energy fluxes were varied from 500 to 1200 W/cm^2 giving rise to heating rates on the order of 10^5 K/s. Heating pulse times were varied from 3 to 10 ms. The ambient gas was 1 atmosphere of air.

Photographic records of the volatile evolution and particle swelling that accompany devolatilization were obtained using a high-speed 16 mm movie camera which was operated at 5000 frames per second. Timing marks were recorded on the film to accurately determine the film speed and to mark the initiation of the heating pulse. As reported elsewhere,[10] these movies provided excellent time resolution of the particle response including rotation and swelling, and definition of distinct stages of the devolatilization process such as heavy (condensible) volatile evolution.

Changes in particle size and temperature that accompany rapid heating were measured using a novel imaging system and a single wavelength radiation pyrometer. The imaging system was developed around a 16 x 62 element silicon photodiode array. Particles were backlit with a HeNe laser and a magnified shadow image was projected onto the detector array. The full array was scanned at 6300 Hz yielding an analog output proportional to the particle cross-sectional area. A 7 percent reflecting beam splitter was placed in line between the focussing optic and the imaging system array to deflect part of the particle image onto a video camera detector. The video camera was employed to facilitate particle capture and positioning in the EDB.

The radiant power emitted from hot particles was measured using a single wavelength optical pyrometer which was filtered to provide a 100 nm bandpass centered at 1.5 μm wavelength. These measurements were made along the same line of sight as the particle size measurements by employing a set of dichroic beam splitters to separate the HeNe backlight laser from the near infra-red radiation required for the pyrometer. Particle temperatures were determined based on measurements of particle size and radiant emission intensity with application of the Wien approximation to Plank's law. Emissivities used in these calculations were estimated based on measurements' and on available literature.[11] Details of the temperature measurement system including pyrometer calibration, data analysis and associated measurement errors are published elsewhere.' A schematic of the measurement system is provided in Figure 1.

Analog outputs from the imaging system, the pyrometer and a heating beam synchronization pulse were acquired using a Data Translation DT2828 interface card in an AT compatible PC. Data acquisition was triggered from the movie camera, when a framing rate of 5000 per second was achieved, and continued at a rate of 10 kHz per channel for a period of 50 ms. Heating pulses were initiated 15.5 ms after initiation of data acquisition. Measurements were made on individual particles of Spherocarb (Foxboro, Analabs), a spherical, microporous molecular sieve carbon and PSOC 1451D a HVA Pittsburgh seam bituminous coal. Ultimate analysis for the carbon sample yielded 95.2 percent carbon, 0.4 percent hydrogen, and 0.7 percent nitrogen.

Ultimate analysis of the coal yielded 83.3 percent carbon, 5.4 percent hydrogen, and 1.6 percent nitrogen on a dry ash free basis.

ANALYSIS

Measured temperature histories were compared with theoretical estimates of the temperature response of radiatively heated particles. Temperature histories were modeled assuming that particles were spherical, heat flow was in the radial direction only, and the incident heating pulses were absorbed and distributed uniformly at the particle surface. Under these assumptions, the transient temperature distribution in the particles was obtained by solution of the Fourier equation for a sphere:

$$\rho_p C_p \frac{\partial T}{\partial t} = K \left(\frac{\partial^2 T}{\partial r^2} + \frac{2}{r} \frac{\partial T}{\partial r} \right) \qquad (1)$$

where ρ_p, C_p, T, K, and r represent particle density, heat capacity, temperature, thermal conductivity and radius, and t represents time. In solving equation 1, the following boundary conditions were applied:

(i) The initial condition at t = 0:

$$T(r,0) = T_0 \qquad 0 \leq r \leq R \qquad (2)$$

(ii) The symmetry condition at the center r = 0:

$$\frac{\partial T(0,t)}{\partial r} = 0 \qquad t \geq 0 \qquad (3)$$

(iii) The energy delivered at the surface r = R:

$$K \frac{\partial T}{\partial r} = \frac{\alpha I}{2} - [\, h(T_s - T_\infty) + \sigma\varepsilon(T_s^4 - T_\infty^4) \,] \qquad (4)$$

where α, I, h, σ and ε represent particle absorptivity, incident radiation flux, heat transfer coefficient, Stefan-Boltzman constant and particle emissivity respectively. The subscripts s and ∞ denote the particle surface and ambient environment.

Equation 1 was solved numerically using an implicit Crank-Nicholson scheme. Calculations were performed using the Merrick model[12] to estimate particle heat capacities. Thermal conductivities were estimated using the temperature data for coals and chars of Badzioch and coworkers.[13] The heat transfer coefficient at the particle surface was calculated assuming a Nusselt number of 2. Calculations were performed employing both a constant particle size assumption and using the measured particle size history as input to the model.

RESULTS

Experiments were conducted with carbon spheres to evaluate the capabilities of the measurement system and to test the validity of the heat transfer analysis. Previous experience with Spherocarb particles indicated sufficient temperature measurement accuracy and response to enable heat capacity measurements of individual particles in the EDB system.[9] Temperature traces for replicate experiments with three different Spherocarb particles are presented in Fig. 2. Heating pulse intensities

for the three experiments varied from 1100 to 1160 W/cm^2 with particle diameters ranging from 135 to 140 μm. The temperatures reported were determined using the pyrometer output and the measured particle size data assuming a particle emissivity of 0.85. The measured temperature histories for the three particles were all very similar with less than 50 K deviation at any given time during the particle heat up. The temperature histories showed a steady rise from 850 K (low temperature limit of pyrometer) up to a temperature around 1200 K and then exhibited a marked decrease in the rate of temperature rise at about 6.5 ms into the heating pulse. Analysis of the corresponding high speed movie records indicated that each of the particles passed through a plastic transition during heat up and showed clear signs of volatile evolution and fragmentation from the surface. The observed change in heating rate coincided with the initiation of volatile evolution and particle fragmentation.

The solid line in Fig. 2 represents the calculated temperature history at the surface of a 135 μm particle exposed to an incident flux of 1160 W/cm^2. Excellent agreement was obtained between temperature measurements and predictions with less than 50 K temperature difference being observed over the first 6.5 ms of particle heating. Beyond 6.5 ms the model predictions exceeded the measured temperature rise. Possible causes for the marked decline in the observed particle heating rate and the corresponding deviation from the predicted temperature rise include; a) thermochemical or thermophysical heat requirements which may be associated with volatile evolution and particle fragmentation, but were not accounted for in the calculations; b) attenuation of the particle emission due to the presence of the volatile aerosol cloud and/or small particle fragments; and, c) attenuation of the heating pulse due to the presence of the volatile cloud or particle fragments around the particle. Efforts are in progress to resolve this issue. The data shown in Fig. 2 are typical in terms of measurement reproducibility and agreement between model predictions and measurements for experiments conducted over a range of Spherocarb particle sizes (125 to 150 μm) and incident heat fluxes (500 to 1200 W/cm^2).

Measured temperature histories from six independent experiments with PSOC 1451D coal are presented in Fig. 3. Initial particle diameters for these experiments ranged from 110 to 127 μm , with heating pulse intensities and times varying from 1040 to 1100 W/cm^2 and 3 to 10 ms respectively. The temperatures reported represent data collected before the particles began to move out of the measurement focal volume. The six data sets, recorded at essentially identical heat input rates, but for different heating times, illustrate that the temperature rise was very similar in each case. The data indicate an initial heating rate on the order of 2.5 x 10^5 K/s to a temperature around 1400 K. For the particles that remained in the detection volume through the duration of the heating pulse, the temperature remained at a plateau value near 1400 K for the last several ms of heating. Analysis of the corresponding high speed movies showed rotation of particles beginning between 1.6 and 1.8 ms into the heating pulse at measured surface temperatures around 900 K. Similar observations of particle rotation were reported previously by Phuoc and Maloney[10] and are most likely associated with the inception of light (non-condensible) volatile evolution. Between 3 and 4 ms into the heating pulse, the first indications of a condensed volatile cloud were observed around the particles, afterwhich intense volatile evolution proceeded. Figure 4 illustrates particle size histories showing the swelling behavior of three particles. These data correspond with three of the temperature records shown in Fig. 3. Most of the observed particle swelling occurred between 3 and 5 ms with the maximum swelling values varying from 10 to 30 percent for the particles studied. During the last 5 or 6 ms of heating, in the longer pulse time experiments, the measured temperatures remained fairly constant at about 1400 K. At the present time it is not clear if this behavior is real or the result of interference from the volatile cloud that forms around the particle during the latter stages of devolatilization. This matter is

the subject of an ongoing investigation. The discussion below, therefore, is limited to the first 4 ms of the particle heat up until this issue can be resolved. It should be noted that intense volatile evolution continued during the last half and for several ms beyond the completion of the heating pulse in the 10 ms duration experiments.

Comparisons of one of the temperature records presented in Fig. 3 with temperature history predictions based on the heat transfer analysis described above are presented in Fig. 5. The base case for the analysis included an initial coal density of 1.2 g/cm^3, and particle emissivity and absorptivity of 0.8. The base case analysis gave poor agreement with the measured temperature histories using the same coal property correlations and initial assumptions that gave good agreement for the carbon spheres heating under similar incident heat flux conditions. A second comparison was made assuming an emissivity of one for the coal particles. As shown in Fig. 5 this modification did improve the agreement between the predicted temperature rise and the measurements, however, the agreement was still poor when compared with the results obtained for carbon spheres. The comparisons in Fig. 5 have significant implications because they suggest that the coal particles heated much faster than predicted based on commonly employed approaches to modeling heat transfer using assumptions routinely applied to coal. Fletcher[3] recently reported that the same coal studied here heated as much as 40 percent faster in an entrained flow reactor than predicted using a fairly comprehensive heat transfer analysis. He used a "corrected" characteristic heat transfer time to obtain good agreement between model predictions and particle temperature measurements. The results presented in Fig. 5 are similar to Fletchers observations and suggest significant errors in the assumed particle properties or model assumptions because, even when assuming all of the incident energy was absorbed by the particle, the measured temperature rise greatly exceeded the model predictions. This observation implies one or more of the following; a) significant temperature gradients existed in the particle, i.e. assumed thermal conductivities for the coal were too high; b) assumed particle thermal mass was too high, i.e. particle density and/or heat capacity were overestimated; and, c) the spherical particle assumption was inadequate to model heat transfer for coal particles, i.e. surface to mass ratios for coal particles significantly exceed that of a sphere.

Additional calculations were performed to evaluate the sensitivity of temperature history predictions to changing particle properties such as heat capacity and thermal conductivity. Some improvements were obtained in the model predictions relative to the measurements when lower heat capacity and thermal conductivities were employed in the analysis. However, there were still significant differences between measurement and prediction if coal property values were held within a range that is generally accepted. Additional improvements in the model predictions might be obtained if mass loss during particle heat up were accounted for in the particle energy balance. No attempt was made to do so, however, because there was no evidence of significant mass loss from the coal particles during the first 3 to 4 ms of particle heating. Attempts were made to estimate the relative contribution to the energy balance due to particle oxidation. Based on these calculations it was concluded that heat release due to oxidation during the initial 4 ms of particle heating was insignificant and should have little influence on the observed particle temperatures. This conclusion is supported by other evidence as well because, if the high heating rates observed resulted from oxidation the associated heat release would lead to particle ignition. No evidence of particle ignition was observed and following the heating pulse, the particles were observed to cool rapidly.

An alternative explanation for the high heating rates observed in the experiments arises from the irregular shape of the coal particles. As is typical when modeling coal behavior, the heat transfer analysis was based on an assumption of spherical particle shape. This analysis gave good agreement with experiments performed on

spherical particles. The mass per unit surface area is an important factor in the analysis and irregular shaped particles may not be dealt with adequately. For example, a cube has a mass per unit surface area approximately 40 percent less than a sphere of equivalent surface area. This may have a significant impact on the energy balance and could account for some of the errors in the predicted particle heating rate.

CONCLUSION

A novel imaging system was developed and applied to study changes in coal particle size and temperature during the early stages of devolatilization at heating rates representative of high intensity combustion processes. Based on these measurements, it is concluded that coal particles heat significantly (on the order of 50 percent) faster than is predicted using commonly employed approaches to model heat transfer. Potential causes for the differences between measured and predicted temperature histories include inadequate understanding of the temperature dependence of relevant coal thermodynamic and heat transfer properties and failure to account for particle shape factors. Regardless of the cause, heat transfer analyses employing spherical particle assumptions and widely accepted coal property correlations may yield significant errors in temperature histories and corresponding errors in the associated devolatilization time scales. Efforts are now in progress to address some of these issues.

ACKNOWLEDGEMENT

This work was funded through the U. S. Department of Energy Advanced Research and Technology Development Direct Utilization Program. E. R. Monazam would like to acknowledge Oak Ridge Associated Universities for their support in the form of a post-doctoral fellowship. The authors also wish to acknowledge the contributions of G. E. Fasching, K. Renner, J. D. Thornton and H. Lemley.

REFERENCES

1. Howard, J. B.: Chemistry of Coal Utilization (M. A. Elliot, Ed.) Second Supplementary Volume, p. 665, John Wiley, 1981.

2. Solomon, P. R. and Hamblen, D. G.: Chemistry of Coal Conversion (R. H. Schlosberg, Ed.) pp. 121-251, Plenum Press, 1985.

3. Solomon, P. R., Serio, M. A., Carangelo, R. M. and Markham, J. R.: Fuel **65**, 182 (1986).

4. Best, P. E., Carangelo, R. M., Markham, J. R. and Solomon, P. R.: Combustion and Flame **66**, 47 (1986).

5. Fletcher, T. H.: Combust. Sci. and Tech. **63**, 89 (1989).

6. Fletcher, T. H.: Combustion and Flame **78**, 223 (1989).

7. Freihaut, J. D. and Proscia, W. M.: Energy and Fuels **3**, 625 (1989).

8. Maloney, D. J., Fasching, G. E., Lawson, L. O. and Spann, J. F.: Rev. Sci. Instrum. **60**, 450 (1989).

9. Monazam, E. R., Maloney, D. J. and Lawson, L. O.: Rev. Sci. Instrum. **60**, 3460 (1989).

10. Phuoc, T. X. and Maloney, D. J.: Twenty-Second Symposium (International) on Combustion, p. 125, The Combustion Institute, 1988.

11. Baxter, L. L., Fletcher, T. H. and Ottesen, D. K.: Energy and Fuels **2**, 423 (1988).

12. Merrick, D.: Fuel **62**, 540 (1983).

13. Badzioch, S., Gregory, D. R. and Field, M. A.: Fuel **43**, 267 (1964).

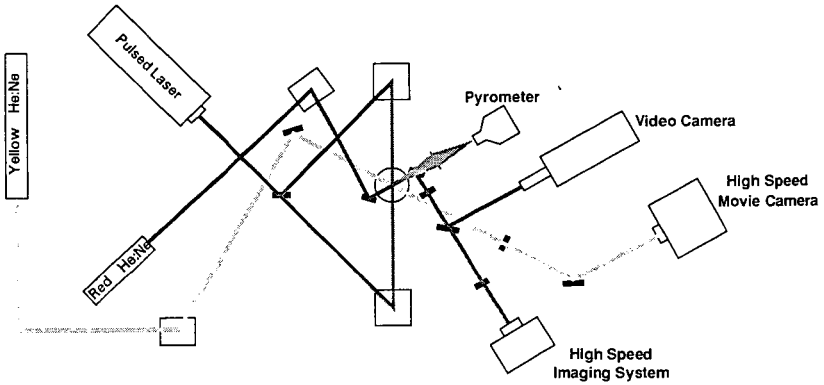

Figure 1. Diagram of EDB Measurement System

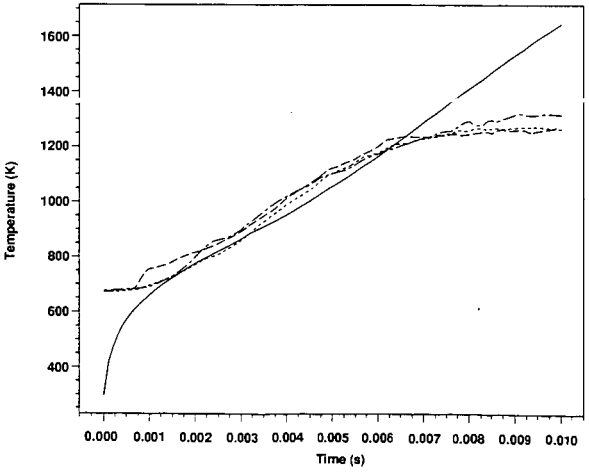

Figure 2. Comparison of Measured Temperature Histories and Model Predictions for Carbon Spheres

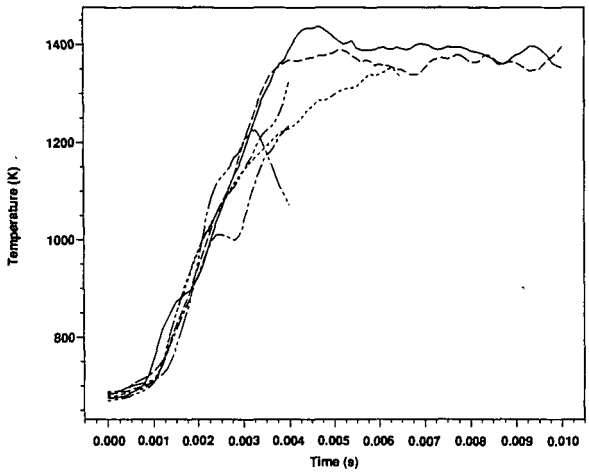

Figure 3. Measured Temperature Histories for Six Coal Particles at Similar Incident Heat Flux Conditions.

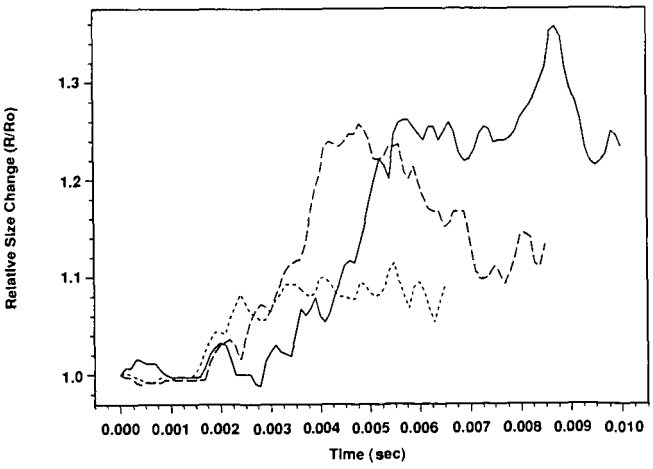

Figure 4. Measured Particle Size Histories for Three Coal Particles at Similar Incident Heat Flux Conditions.

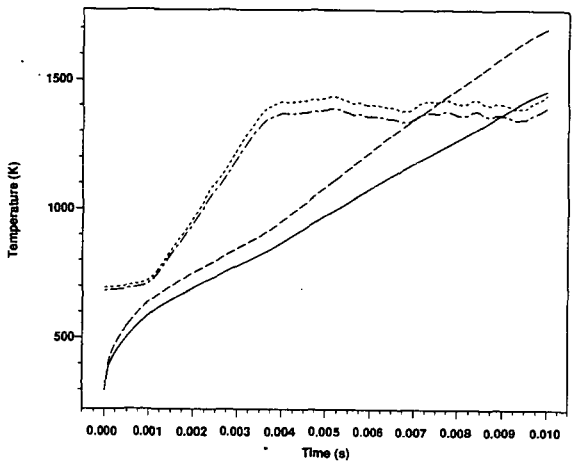

Figure 5. Comparisons of Measured and Predicted Temperature Histories for a Coal Particle as a Function of Assumed Particle Emissivity.
ε = 0.8: ------- Measured, ——— Predicted
ε = 1.0: — - — - — Measured, — — — Predicted